npg

The DNA repair complex Ku70/86 modulates *Apaf1* expression upon DNA damage

D De Zio[1,2], M Bordi[1,2], E Tino[2], C Lanzuolo[3,4], E Ferraro[2], E Mora[2], F Ciccosanti[5], GM Fimia[5], V Orlando[3] and F Cecconi*,[1,2]

Apaf1 is a key regulator of the mitochondrial intrinsic pathway of apoptosis, as it activates executioner caspases by forming the apoptotic machinery *apoptosome*. Its genetic regulation and its post-translational modification are crucial under the various conditions where apoptosis occurs. Here we describe Ku70/86, a mediator of non-homologous end-joining pathway of DNA repair, as a novel regulator of Apaf1 transcription. Through analysing different Apaf1 promoter mutants, we identified an element repressing the Apaf1 promoter. We demonstrated that Ku70/86 is a nuclear factor able to bind this repressing element and downregulating Apaf1 transcription. We also found that Ku70/86 interaction with Apaf1 promoter is dynamically modulated upon DNA damage. The effect of this binding is a downregulation of Apaf1 expression immediately following the damage to DNA; conversely, we observed Apaf1 upregulation and apoptosis activation when Ku70/86 unleashes the Apaf1-repressing element. Therefore, besides regulating DNA repair, our results suggest that Ku70/86 binds to the Apaf1 promoter and represses its activity. This may help to inhibit the apoptosome pathway of cell death and contribute to regulate cell survival.
Cell Death and Differentiation (2011) **18,** 516–527; doi:10.1038/cdd.2010.125; published online 22 October 2010

Apaf1 is a crucial factor in regulating the mitochondrial apoptotic pathway. Apaf1 normally being in an inactive conformation, its oligomerization is caused by cytochrome *c* release from mitochondria, after apoptotic stimuli, in the presence of dATP/ATP.[1] Seven Apaf1 molecules generate the apoptosome,[2,3] which is able to recruit the procaspase 9 and allow its activation.[4] In such a multimeric complex, the apoptosome activates executioner caspases, which orchestrate the 'safe' destruction of the cell.[5]

Apaf1 is regulated at several levels. As regards the transcriptional control, it is well established as being positively regulated by p53[6,7] and E2F1,[8] factors involved in apoptosis and cell cycle regulation. It has been demonstrated that p53 recognizes and binds two sites on the human promoter of Apaf1,[8] and that this interaction seems to be enhanced by Zac-1, a transcription factor involved in the induction of G1 arrest.[9] In addition, E2F1 has been reported to induce apoptosis by directly activating Apaf1.[10] Regarding epigenetic regulation, Apaf1 promoter seems to be silenced by methylation in several tumours (albeit this finding is still controversial in some cases).[11–14] Histone deacetylase (HDAC) inhibition activity restores the Apaf1 expression in mouse developing retina;[15] this was also observed in developing but not in mature neurons, unless E2F1 was concomitantly expressed.[16] In particular, HDAC inhibition resulted in an increased binding of E2F1 and p53 to the Apaf1 mouse promoter.[15] Moreover, different Apaf1 levels correlated with differences in the levels of E2F1 and were found to be critical for allowing cytochrome *c* to induce apoptosis in brain tumours but not in normal tissues.[17]

Being a positive regulator of the apoptotic cell death, Apaf1 transcriptional regulation is crucial under the various conditions where apoptosis occurs, such as in driving development, controlling tissue homeostasis and preventing the propagation of DNA-damaged cells.

The main damage to DNA helices is the double-strand break (DSB), which is essentially repaired by the non-homologous end-joining (NHEJ) pathway.[18] This repairs the DNA by a homology-independent mechanism rejoining broken ends irrespective of the sequence. Upon exposure to different genotoxic insults, the Ku70/86 heterodimer (Ku) binds to the DNA broken ends and recruits the catalytic subunit of the DNA-dependent protein kinase (DNA-PKcs). The formation of this complex results in the subsequent recruitment and phosphorylation of other proteins, such as XRCC4, DNA Ligase IV, Cernunnos/XLF and Artemis so as to ligate the DNA broken ends.[19] Ku seems to be critical for cell survival, as the failure of the cells to carry out DNA repair results in an apoptotic response. The Ku70 and Ku86 proteins were originally found as a major target of auto-antibodies taken from Japanese patients with scleroma-polymyositis overlap syndrome.[20] Current knowledge on Ku deals with its

fundamental role in DNA repair, but it is also implicated in other cellular processes, including telomere maintenance, antigen receptor gene arrangements (VDJ recombination), regulation of specific gene transcription and apoptosis.[19] Indeed, Ku70 can sequester Bax from the mitochondria and mediate Bax de-ubiquitylation.[21] Regarding its transcriptional function, Ku has been reported to act in both a sequence-nonspecific and -specific manner. This factor has been found to be associated with RNA polymerase II elongation sites without a sequence-specific DNA binding.[22] On the other hand, there are several reports indicating that Ku acts as a transcription factor: for example, in the repression of the human α-myosin heavy-chain promoter during heart failure;[23] or in contributing the oncogene ERBB2 overexpression in breast cancer cells by interacting with activator protein-2 transcription factors.[24]

In this report we analyse the transcriptional regulation of murine Apaf1 and we demonstrate a functional interaction between Ku70/86 heterodimer and a specific region of Apaf1 promoter. We find that Ku acts as transcription repressor, leading to a downregulation of Apaf1 expression. In particular, our findings suggest that, upon DNA damage, Ku exerts a pro-survival role not only through repairing DNA damage, but also contributing to modulate Apaf1 expression.

Results

Analysis of murine Apaf1 promoter activity. To investigate the transcriptional modulation of murine Apaf1, we focused on a 7 kb region of the Apaf1 promoter (-4210) (Figure 1a). We generated three deletion constructs ($\Delta -1509$; $\Delta -589$; $\Delta +305$) (Figure 1a) and placed them upstream of the firefly luciferase cDNA, in order to compare their activity and to identify relevant regions for transcriptional regulation. These constructs were transfected in different cell types ($B_{16}F_{12}$, murine melanoma cells; $C_3H_{10}T_{1/2}$, murine fibroblasts; ImimPc-2, human pancreatic primary solid tumor cells; and ETNA, Embryonic Telencephalic Naïve Apaf1 cells), and the relative promoter activities were measured. As reported in Figure 1b–e, one of the constructs ($\Delta -589$) shows a significant increase in promoter activity when compared with the whole promoter in each cell line analysed. The constructs $\Delta -1509$ and -4210 have
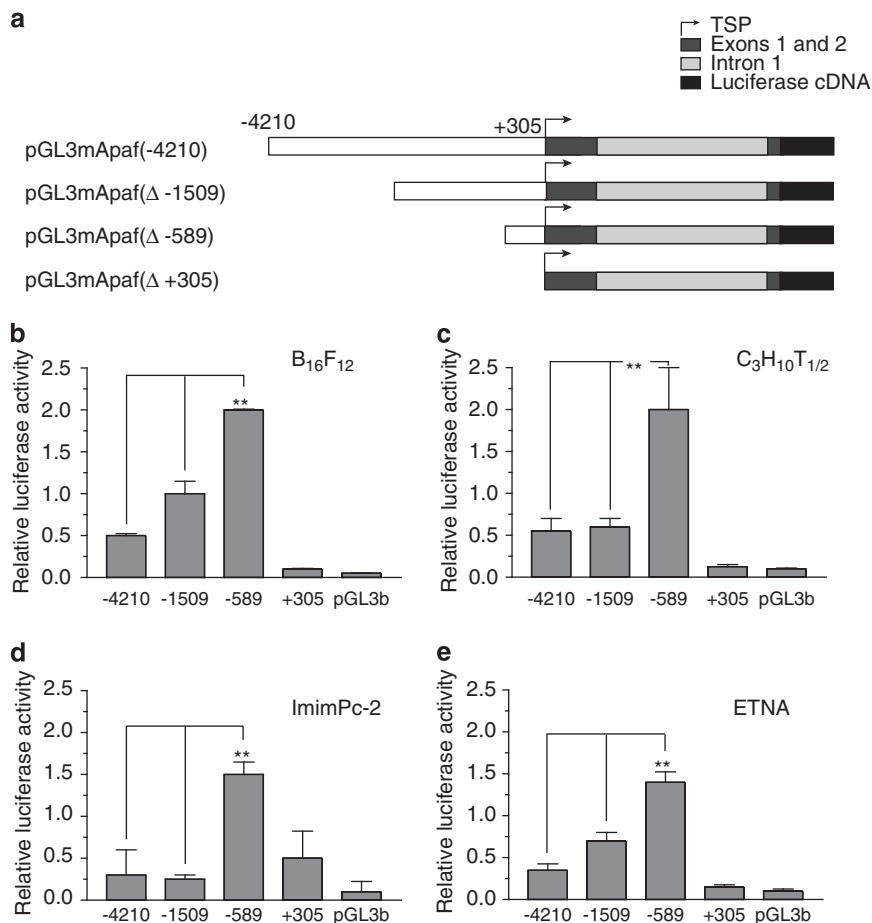
Figure 1 Analysis of murine Apaf1 promoter activity. (**a**) A schematic representation of the region of 7 kb containing the murine Apaf1 promoter (-4210) and its deleted variants ($\Delta -1509$, $\Delta -589$ and $\Delta +305$), cloned upstream of the firefly luciferase cDNA in pGL3-basic, is shown. TSP, transcription start point. (**b–e**) The complete promoter containing the vector (-4210), the deletion constructs ($\Delta -1509$, $\Delta -589$ and $\Delta +305$) and the empty vector (pGL3b), were transfected in different cell lines: $B_{16}F_{10}$ (**b**), $C_3H_{10}T_{1/2}$ (**c**), ImimPc-2 (**d**) and ETNA (**e**). The relative luciferase activity was measured 24 h after transfection and was reported as the ratio of the firefly luciferase activity and renilla luciferase activity. Average activities $\pm$ S.D. of three independent experiments with duplicate samples are shown; $^{**}P \leq 0.01$
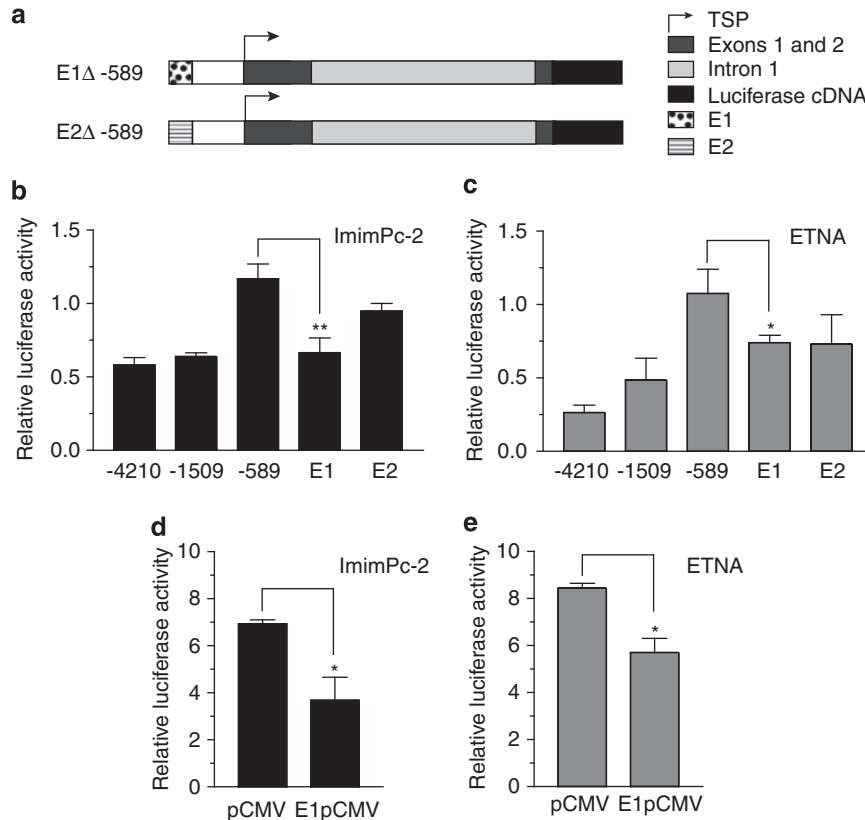
Figure 2 Identification of E1 as the minimal region able to reduce both Apaf1 and CMV promoter activities. (**a**) The constructs E1Δ −589 and E2Δ −589 were generated to test the ability of two regions of about 50 bp (E1 and E2, between −1509 and −1402) in reducing the activity of Δ −589 construct. (**b** and **c**) E1 and E2 construct activities were compared with that of −4210, Δ −1509 and Δ −589, by transfecting ImimPc-2 (**b**) and ETNA (**c**) cells and determining luciferase activity as described in the previous experiments. (**d** and **e**) E1 was cloned upstream the control promoter Cytomegalovirus (CMV), which controls the firefly luciferase expression in pGL3-basic plasmid, to test the ability of E1 sequence in reducing CMV promoter activity (E1pCMV). ImimPc-2 (**d**) and ETNA (**e**) cells were transfected with E1pCMV or pCMV and activities were compared. Average activities ± S.D. of three independent experiments with duplicate samples are shown; *$P \leq 0.05$, **$P \leq 0.01$

comparable activities whereas, as expected, the construct Δ +305 shows an activity comparable with that of the pG13-basic empty vector, as it lacks the minimal regions required for transcription. On the basis of this observation, we hypothesized the existence of a promoter regulatory element in a region of about 1000 bp. This element is located between nucleotides −1509 and −589 and is able to repress Apaf1 promoter activity.

Identification of the repressing element on Apaf1 promoter. To identify the smallest region able to suppress Apaf1 expression, we generated an additional series of deletion constructs (referred as 1–7) (Supplementary Figure 1) and transfected them in the ImimPc-2 and ETNA cell lines. We found that a region of about 110 bp, located between Δ −1509 and Δ −1402, was involved in promoter repression. Indeed, all the constructs that did not contain this fragment, displayed a higher activity than that observed for −4210 and Δ −1509 (Supplementary Figures 1B and C). Therefore, this region should reasonably include the site able to repress Apaf1 promoter activity. We divided the fragment between −1509 and −1402 into two regions, E1 and E2, each about of 50 bp, and cloned them upstream of the construct Δ −589 (Figure 2a) to verify their ability to modulate normal promoter

activity. Region E1 significantly decreased Δ −589-promoter activity in ImimPc-2 and ETNA cells, whereas E2 only partially reduced such activity in ETNA (Figure 2b and c).

In addition, we cloned E1 upstream of a control promoter, pCMV (E1pCMV). We compared the activity of the two constructs (pCMV and E1pCMV) so as to test the ability of this region to act as an autonomous repressor element. Our analyses showed that the presence of E1 significantly decreased pCMV activity in both the cell lines analysed (Figure 2d and e). Moreover, *in silico* analysis performed by the multiple alignment of the E1 region against Apaf1 promoter sequences of different organisms revealed a high conservation of this sequence in mammals (Supplementary Figure 2). Taken together, these data indicate that E1 could represent a novel-repressing element involved in Apaf1 transcriptional regulation.

Ku70/86 binds Apaf1 promoter *in vitro*. To identify factors involved in the activity of this repressor, we performed an electrophoretic mobility shift assay (EMSA). By incubating nuclear extracts from ImimPc-2 and ETNA cells with a radioactively labelled E1 oligonucleotide, we observed a supershift band in both samples (Figure 3a). This suggests that the E1 fragment is recognized and bound by some
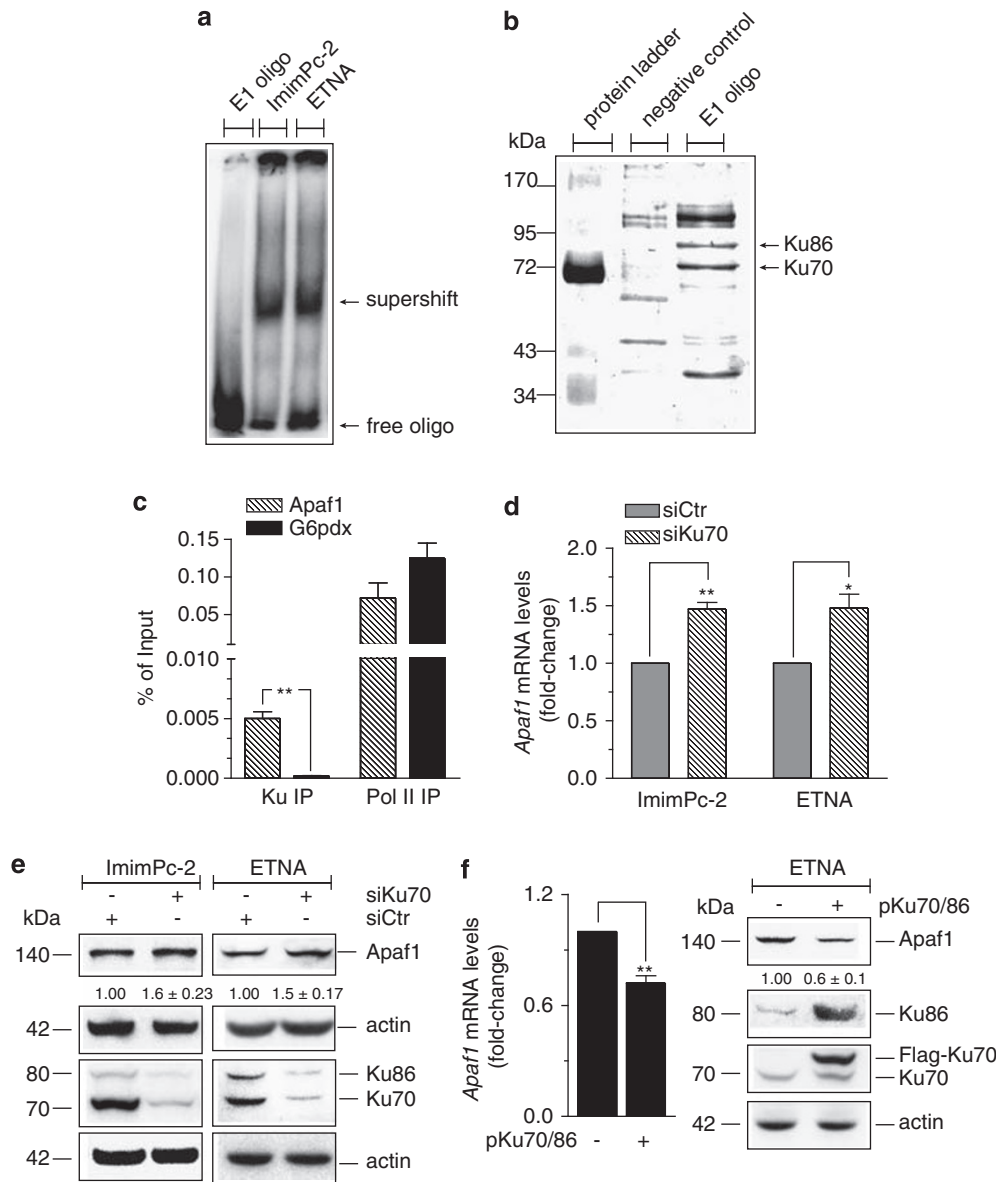
Figure 3 *In vitro* and *in vivo* interaction between Ku70/86 and murine Apaf1 promoter. (**a**) EMSA assay was performed using nuclear extracts from ImimPc-2 and ETNA cells and E1-labelled oligonucleotides. The first lane shows E1 oligonucleotides alone as negative control. (**b**) DNA pull-down was carried out using ETNA cell extracts and E1 oligonucleotides (lane 3) or negative control oligonucleotides (lane 2). The arrows indicate proteins eluted with E1 oligonucleotides and not isolated with control oligonucleotides and analysed by MALDI-TOF/TOF (Ku70 and Ku86 proteins). (**c**) ChIP assay was carried out in ETNA cells. Cross-linked cell lysates were sonicated and immunoprecipitated by anti-RNA polymerase II (Pol II IP), anti-Ku (Ku IP) and no antibody. The immunoprecipitated DNA was analysed by quantitative real-time PCR using oligonucleotides specific for the target sequence of Apaf1 promoter. G6pdx oligonucleotides were used as control in Pol II- and Ku-immunoprecipitated samples. Histograms show the percentage of input of the immunoprecipitated chromatins. Each value was shown as the mean ± S.E.M.; $n = 3$, **$P \leq 0.01$. (**d** and **e**) ImimPc-2 and ETNA cells were transiently transfected with siRNA duplex against human and murine Ku70 mRNA target sequences (siKu70) and with a scramble siRNA duplex (siCtr). (**d**) Cells transfected for 72 h were assayed for *Apaf1* mRNA by quantitative real-time PCR. mRNA levels were normalized to *GAPDH* and β-actin mRNAs, used as internal control. Data display the fold-changes of *Apaf1* mRNA relative to control cells, which is arbitrary set as one, and were shown as the mean ± S.E.M.; $n = 3$, *$P \leq 0.05$, **$P \leq 0.01$. (**e**) After 72 h of transfection with siKu70 or siCtr, ImimPc-2 and ETNA cells were assayed for Ku70, Ku86 and Apaf1 protein levels. (**f**) pKu70- and pKu86-transfected ETNA cells were analysed for Ku70 and Ku86 protein levels after 24 h of transfection. Empty vector-transfected ETNA cells were used as control (−). Quantitative real-time PCR and immunoblot were carried out in 24 h-transfected ETNA cells to evaluate *Apaf1* mRNA (as above described) and protein levels. Immunoblots reported are from one experiment representative of three that gave similar results. Density of immunoreactive bands was calculated using the software AlphaEaseFC (Alpha-Innotech, Santa Clara, CA, USA), normalized for actin and reported as arbitrary units (shown as the mean ± S.D.)

nuclear factors, which probably act as repressors of Apaf1 transcription. To detect these putative factors, we carried out a DNA pull-down assay. Biotinylated double-stranded oligonucleotides containing the E1 sequence or an unrelated one, as a negative control, were associated to streptavidine-coated beads and allowed to react with nuclear extracts from ETNA cells. Bound proteins were eluted using an excess of free oligonucleotides and analysed by SDS-PAGE. After

Table 1 MALDI-TOF/TOF identifications

Protein name	Swiss prot entry	Mascot score	No. masses matched	No. masses not matched	% Sequence coverage	MW calculated	MW observed
ATP-dependent DNA helicase II, 80 kDa subunit (Ku86)	P13010	158	27	40	39	83091.5	90000
ATP-dependent DNA helicase II, 70 kDa subunit (Ku70)	P12956	166	28	40	47	69953.1	72000

SYPRO Ruby staining, two clear bands, corresponding to proteins with apparent molecular weights of 72 and 90 kDa, were detected as specific for E1 binding (see arrows in Figure 3b). The protein bands were excised from the gel, digested with trypsin, and subjected to MALDI-MS/MS for protein identification. As described in Table 1, mass spectrometry analysis identified the two proteins as Ku70 and Ku86.

Ku70/86 binds Apaf1 promoter *in vivo* and represses its transcription. To confirm the interaction between Ku70/86 and Apaf1 promoter *in vivo*, we performed a chromatin immunoprecipitation (ChIP) assay. Cross-linked chromatin from ETNA cells was immunoprecipitated with antibodies against the heterodimer Ku and the RNA polymerase II (Pol II), as a positive control. We found that Ku specifically binds the E1 region of Apaf1 promoter at variance with the negative control G6pdx, as shown in the anti-Ku immunoprecipitated sample subjected to quantitative real-time PCR using Apaf1 promoter oligonucleotides (Figure 3c).

On the basis of these results, we set out to establish the functional role of this interaction. As these proteins function synergically, we analysed the effect of Ku70 silencing on Apaf1 promoter activity (Figure 3d and e). In fact, it has been reported that Ku70-deficient mice exhibit decreased levels of Ku86, and *vice versa*.[25–27] We found that 72 h of transfection are sufficient to efficiently knockdown Ku70/86 (Figure 3e). Quantitative real-time PCR and immunoblotting analyses showed that a significant increase of *Apaf1* mRNA and protein levels occurred both in ImimPc-2 and in ETNA cells when compared with cells transfected for 72 h with an unrelated control oligonucleotide (Figure 3d and e). Conversely, when we transfected ETNA cells with both Ku70 and Ku86 expressing vectors (pKu70/86), we observed a decrease of Apaf1 expression (Figure 3f). Taken together, these data show that Ku70/86 binds Apaf1 promoter and represses Apaf1 expression.

Ku70/86 binds dynamically the Apaf1 promoter and modulates its expression upon DNA damage. As Ku is known to be involved in DNA damage repair, we decided to explore whether Ku/Apaf1 promoter interaction is modulated following induction of DNA damage by hydrogen peroxide or etoposide in ETNA cells. Fluorescence images and immunoblotting analyses displayed the occurrence of histone H2A.X phosphorylation (Figure 4a–c) and the oxidative modification of deoxyguanosine (8-OHdG) (Supplementary Figure 3A and B), which are well-established markers of DNA lesion,[28,29] already after 1 h of hydrogen peroxide or etoposide incubation. This event correlates well with Ku70 accumulation within the nuclei either upon hydrogen peroxide or etoposide

treatment (Figure 4b and c), suggesting that Ku70 had a crucial role in DNA repair process also under our experimental conditions. We then assessed whether this nuclear accumulation was associated with the modulation of Apaf1 expression, focusing on a time window of 6 h when apoptosis was not still executed (Supplementary Figure 4). We found that *Apaf1* mRNA and protein levels were significantly decreased by about 30% with respect to the control in both H_2O_2- and etoposide-treated ETNA cells (Figure 5a and b). Interestingly, after 6 h of treatment Apaf1 levels increased to reach values higher than control cells (Figure 5a and b). To explain these dynamical changes of Apaf1 expression, we investigated the interaction between Ku and the Apaf1 promoter by quantitative ChIP, upon exposure to DNA-damaging treatments. ChIP, together with quantitative real-time PCR, was therefore performed on untreated (−) and H_2O_2-treated ETNA cells (1, 3 and 6 h). By immunoprecipitating with the anti-Ku antibody, we observed an enhancement of Ku/Apaf1 promoter interaction, soon after the first hour of H_2O_2 treatment (Figure 5c). This significantly increased after 3 h of treatment, likely because of maintain Apaf1 transcription at low levels, and backed down to control values after 6 h (Figure 5c). Conversely, quantitative ChIP analyses performed by anti-Pol II antibody, indicated that the RNA polymerase II strongly bound the transcription start-point region of Apaf1 promoter only after 6 h of treatment, in association with the observed increase of *Apaf1* mRNA and protein levels (Figure 5a, b and d). Of note, Pol II is poised on the transcription start region of Apaf1 promoter during the first 3 h of treatment, when Ku binds Apaf1 promoter, and *Apaf1* mRNA levels are significantly decreased, see in Figure 5d. As there are multiple steps between Pol II recruitment on TSP and productive elongation,[30,31] this result could be explained by the fact that Pol II has to be ready for the subsequent activation of Apaf1 transcription.

Moreover, Apaf1 repression is exclusively dependent on DNA damage, as other apoptotic stimuli, such as protein kinase C-inhibition by staurosporine (STS), did not affect Apaf1 transcription through Ku/Apaf1 promoter binding (Supplementary Figure 5).

These data indicate that, upon DNA damage, Apaf1 transcription is dynamically modulated by the Ku complex.

Ku70/86-mediated Apaf1 regulation modulates cell death upon DNA damage. To detect whether Apaf1 modulation mediated by Ku70/86 binding concurred to cell death control, we analysed during a time course the events underlying the mitochondrial pathway of apoptosis after hydrogen peroxide treatment. Analysis of cytochrome *c* subcellular distribution indicated that cytochrome *c* was released from mitochondria
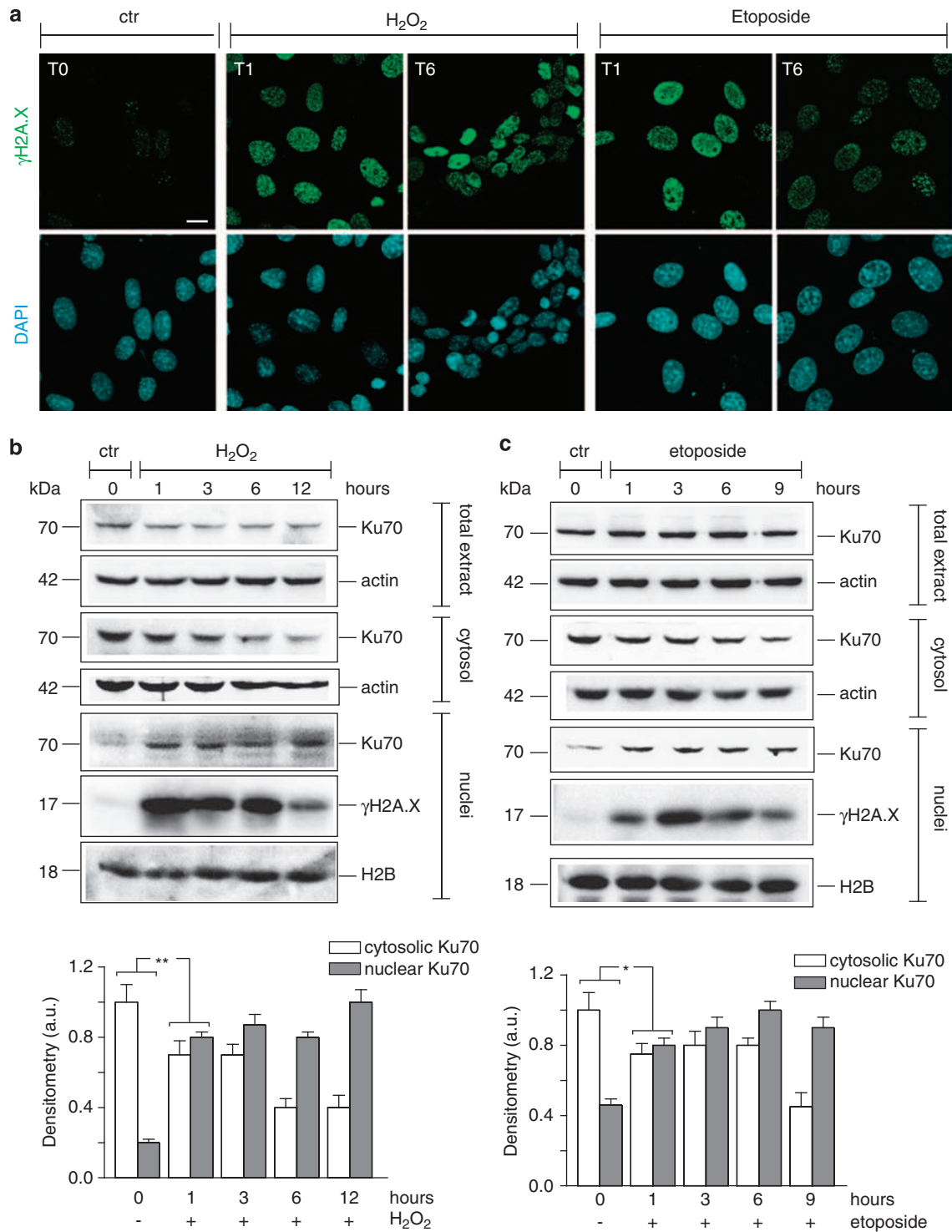
Figure 4 DNA damage induction by hydrogen peroxide and etoposide. (**a**) ETNA cells were left untreated (ctr), treated with hydrogen peroxide (500 μM) for 1 h and then replaced with fresh medium for 1 and 6 h (T1 and T6), or treated with etoposide (20 μM) for 1 and 6 h (T1 and T6). Next, they were fixed and immunostained using an anti-γH2A.X antibody (green), counterstained with DAPI (blue) for the determination of nuclei and then observed by confocal microscopy (scale bar, 10 μm). (**b** and **c**) ETNA cells were left untreated (ctr), treated with hydrogen peroxide (500 μM) for 1 h and then replaced with fresh medium for 1, 3, 6 and 12 h (**b**), or treated with etoposide (20 μM) for 1, 3, 6 and 9 h (**c**). Total, cytosolic and nuclear cell extracts were subjected to SDS-PAGE and analysed for Ku70 (total, cytosolic and nuclear extracts) and γH2A.X (nuclear extracts) protein levels. Actin was used as a loading control for total and cytosolic extracts; H2B was used as a loading control for nuclear extracts. Immunoblots reported are from one experiment representative of three that gave similar results. Densitometric analyses were calculated using the software AlphaEaseFC, normalized for actin (cytosolic fraction) or H2B (nuclear fraction) and reported as arbitrary units (a.u.) and the mean $\pm$ S.D.; *$P \leq 0.05$, **$P \leq 0.01$
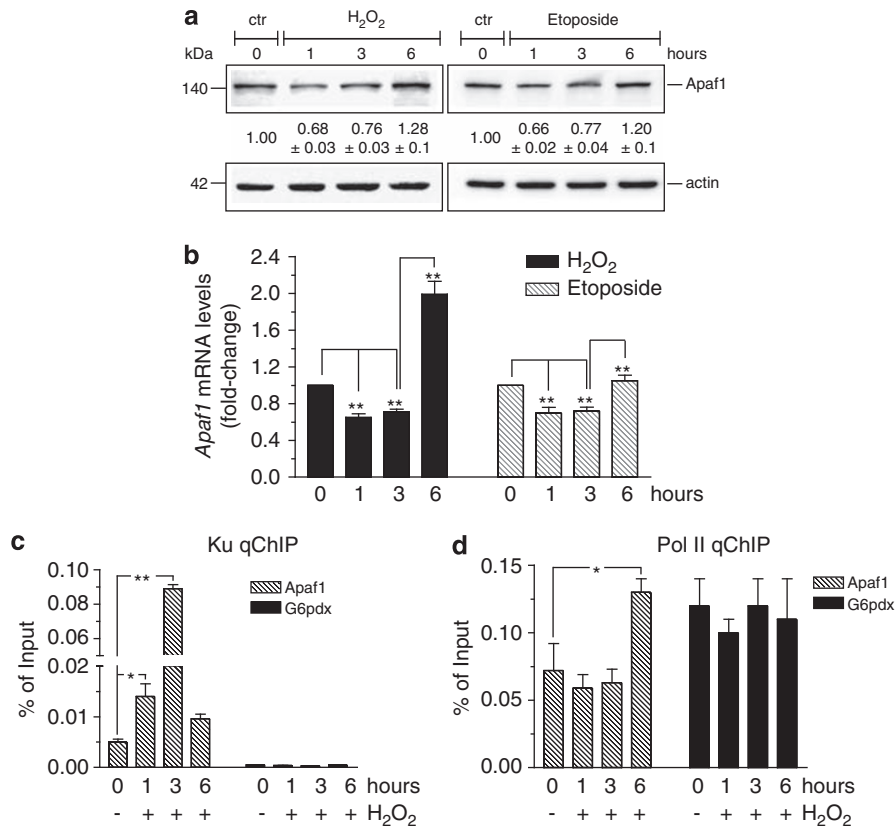
Figure 5 Dynamics of Ku/Apaf1 promoter binding upon DNA damage. (**a–d**) ETNA cells were left untreated (ctr), treated with hydrogen peroxide (500 μM) for 1 h and then replaced with fresh medium for 1, 3 and 6 h, or treated with etoposide (20 μM) for 1, 3 and 6 h. (**a**) Total cell lysates were subjected to SDS-PAGE and analysed for Apaf1 protein level. Actin was used as a loading control. Immunoblots reported are from one experiment representative of three that gave similar results. Density of immunoreactive bands was calculated using the software AlphaEaseFC, normalized for actin and reported as arbitrary units (shown as the mean $\pm$ S.D.). (**b**) The mRNA levels of *Apaf1* were evaluated at each time point by quantitative real-time PCR and were normalized to β-actin, used as internal control. Data display the fold-changes of *Apaf1* mRNA relative to control cells, which is arbitrary set as one, and were shown as the mean $\pm$ S.E.M.; $n = 3$, **$P \leq 0.01$. (**c** and **d**) Cross-linked cell lysates were sonicated and immunoprecipitated by anti-Ku (panel **c**) and anti-Pol II (panel **d**) antibodies. The immunoprecipitated DNA was analysed by quantitative real-time PCR using oligonucleotides specific for the target sequence of Apaf1 promoter (panel **c**) and the region containing Apaf1 TSP (**d**). G6pdx oligonucleotides were used as control in Ku- and Pol II-immunoprecipitated samples. Histograms show the percentage of input of the immunoprecipitated chromatins, from untreated ($-$) and hydrogen peroxide (500 μM)-treated (1, 3, 6 h) ETNA cells. Each value was shown as the mean $\pm$ S.E.M.; $n = 3$; *$P \leq 0.05$, **$P \leq 0.01$

as soon as 1 h after H$_2$O$_2$ administration (Figure 6a). However, caspase 3 was activated only at 6 h of treatment, time at which Apaf1 resulted to be no more inhibited (Figure 6a), suggesting that the downregulation of Apaf1, occurring early upon DNA damage, had a role in the inhibition of caspase-3 cleavage, even in the presence of cytosolic cytochrome *c*.

Moreover, under conditions of Ku downregulation by siKu70 transfection in ETNA cells, the decrease of *Apaf1* mRNA and protein levels was not observed upon hydrogen peroxide treatment (Figure 6b–d). In contrast, the protein levels of Apaf1 and cleaved caspase 3 were greatly enhanced, when comparing siKu70- *versus* siCtr-transfected ETNA cells already after 1 h of treatment (Figure 6c and d). Similarly, under these conditions, cytochrome *c* was released into the cytosol at the same extent both in Ku70-proficient and -deficient ETNA cells (Figure 6c and d). Also, caspase 3 was activated even in the absence of H$_2$O$_2$ (Figure 6c and d). This suggests that Ku depletion can induce an upregulation of Apaf1 expression, which may be sufficient to activate caspase 3.

To further corroborate this assumption, we transfected an Apaf1-expressing vector (pApaf1) lacking E1 regulatory region recognized by Ku70/86, in Apaf1-deficient cells named ETNA$^{-/-}$ cells[32] (Figure 6e and f). Cleaved caspase 3 was already detected as soon as Apaf1 was re-introduced in these cells. Moreover, no significant change of Apaf1 protein and mRNA levels were observed in pApaf1-transfected cells upon H$_2$O$_2$ treatment, although this resulted in DNA damage and, in turn, in the phosphorylation of histone H2A.X. This finding suggests that the downregulation of Apaf1 expression, observed upon DNA damage, mainly depends on the effect of Ku on Apaf1 transcription.

Taken together these data indicate that Ku70/86-dependent modulation of Apaf1 expression contributes to the regulation of the apoptotic pathway occurring upon DNA damage induction.

Discussion

Here we demonstrate that a specific sequence of Apaf1 promoter functions as a repressing element of its activity.
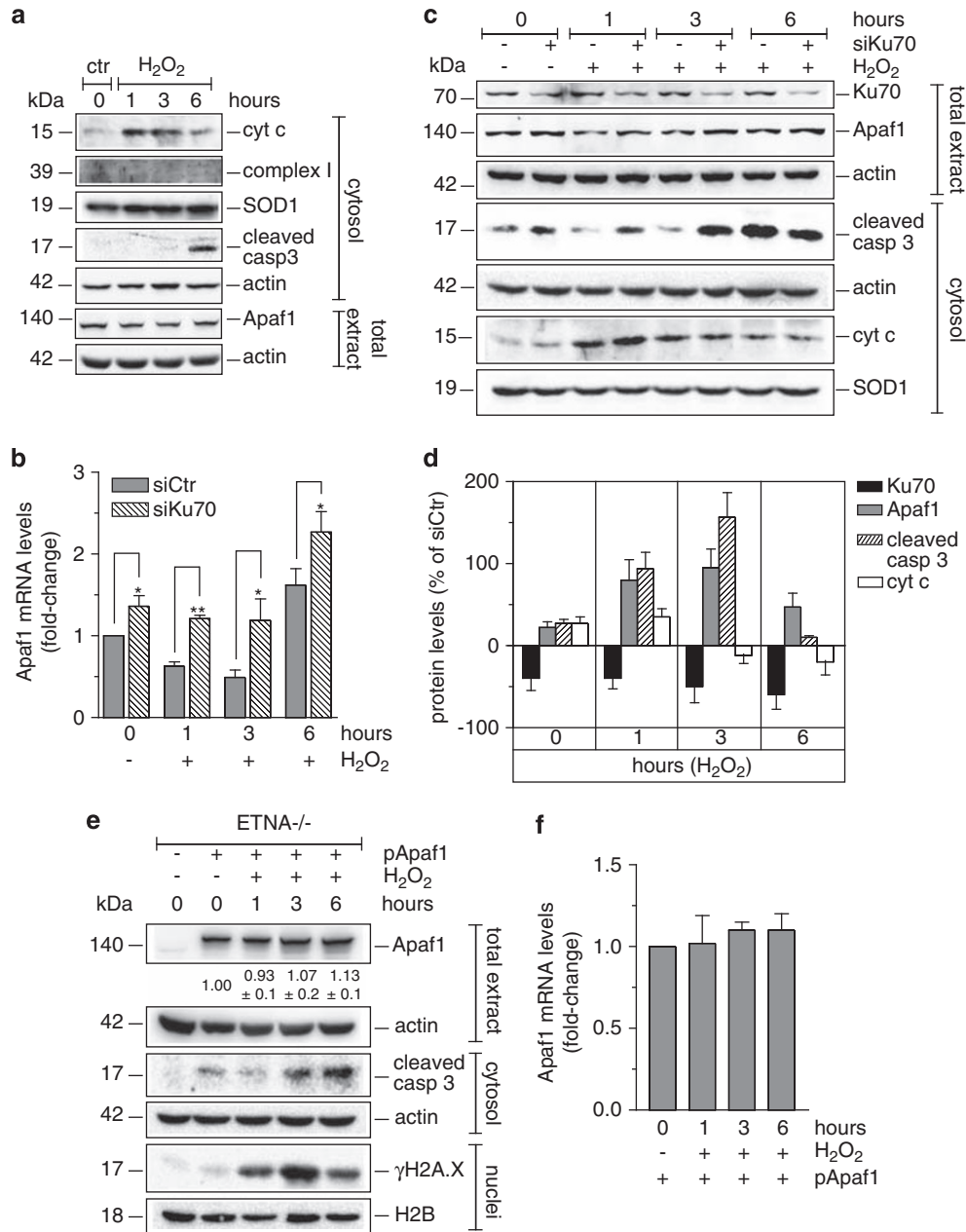
Figure 6 Cell death regulation under Ku and Apaf1 modulation and DNA damage. (**a**) Mitochondrion/cytosol fractionation was performed to assay the presence of cytochrome *c* within the cytosol in untreated (−) or treated with hydrogen peroxide (500 μM) for 1, 3 and 6 h ETNA cells. The 39 kDa subunit of mitochondrial complex I was used as marker of purity. Cu/Zn-SOD (SOD1) was used as marker of the cytosolic fraction. Total cell lysates were analysed for Apaf1 and cytosolic extracts for cleaved caspase-3 protein levels. Actin was used as a loading control. (**b–d**) ETNA cells were transiently transfected with siRNA duplex against murine Ku70 mRNA target sequences (siKu70) and with a scramble siRNA duplex (siCtr). After 72 h of transfection, cells were left untreated (−) or treated with hydrogen peroxide (500 μM) for 1, 3 and 6 h. (**b**) The mRNA levels of *Apaf1* were evaluated at each time point by quantitative real-time PCR and were normalized to β-*actin*, used as internal control. Data display the fold-changes of *Apaf1* mRNA relative to control cells, which is arbitrary set as one, and were shown as the mean ± S.E.M.; $n = 3$, *$P \leq 0.05$, **$P \leq 0.01$. (**c**) Cell lysates were subjected to SDS-PAGE and assayed for Ku70, Apaf1 (total extract) and cleaved caspase-3 (cytosolic extract) protein levels. Actin was used as loading control. Mitochondrion/cytosol fractionation was performed to assay the presence of cytochrome *c* within the cytosol. Cu/Zn-SOD (SOD1) was used as marker of the cytosolic fraction. (**d**) Ku70, Apaf1, cleaved caspase 3 and cytochrome *c* protein levels in siKu70-transfected cells were calculated by densitometric analysis using the software AlphaEaseFC. Each value was normalized for actin or SOD1 and reported as % of siCtr. (**e** and **f**) ETNA$^{−/−}$ cells were transfected with pApaf1-expressing vector or with the empty vector (−) and after 24 h they were left untreated (−) or treated with hydrogen peroxide (500 μM) for 1, 3 and 6 h. (**e**) Apaf1, cleaved caspase 3 and γH2A.X were assayed in the total, cytosolic and nuclear extracts, respectively. Actin and H2B were used as loading controls. Immunoblots reported are from one experiment representative of three that gave similar results. Density of Apaf1 immunoreactive bands was calculated using the software AlphaEaseFC, normalized for actin and reported as arbitrary units (shown as the mean ± S.D.). (**f**) The mRNA levels of *Apaf1* were evaluated at each time point by quantitative real-time PCR using oligonucleotides specific for the C-terminus of *Apaf1* mRNA, which do not anneal to the endogenous *Apaf1/genetrap* fused transcript produced in ETNA$^{−/−}$ cells. Data display the fold-changes of *Apaf1* mRNA relative to control cells, which is arbitrary set as one, and were shown as the mean ± S.E.M.; $n = 3$

In fact, the removal of this sequence is enough to increase Apaf1 promoter activity. Mass spectrometry, chromatin immunoprecipitation assay and silencing experiments have revealed that the heterodimer Ku, composed of Ku70 and Ku86 subunits, can bind to this specific sequence of Apaf1 promoter, negatively regulating its expression.

To date, two transcription factors, E2F1 and p53, have been revealed to regulate Apaf1 in response to several stress factors, thus controlling cell cycle progression.[6–8] E2F1 has been also suggested as having a differential capacity to induce Apaf1 transcription, on the basis of Apaf1 promoter association or not with active chromatin.[16] In particular, it has been demonstrated that Apaf1 promoter is associated with active chromatin in developing neurons and repressed chromatin in mature ones.[16] Apaf1 expression drops dramatically during neuronal differentiation and allows mature neurons to resist cytochrome *c*-dependent apoptosis.[16,17] Our finding that Apaf1 can be repressed by Ku could provide a further explanation to this event, as Ku has been found to be implicated in telomeric silencing by anchoring telomeres to repressed chromatin.[33] Ku could bind the Apaf1 promoter far more in differentiated cells than in proliferating ones, a hypothesis that our experiments in neuronal precursor cells (ETNA cells) support. In fact, we did not observe a strong Ku/Apaf1 promoter interaction in physiological conditions, as Apaf1 has to be expressed at high levels in neuronal progenitors, in order to guarantee the potential of displaying apoptosis. ETNA cells derive, indeed, from the telencephalon of developing brain at embryonic stage 14.5, when massive apoptosis occurs in proliferating neuronal precursors.[34] Nevertheless, in Ku70/86 double-knockout mice, a dramatic increase of cell death has been detected in developing embryonic neurons.[35] This could be in part due to the enhancement of Apaf1 expression in the absence of Ku/Apaf1 promoter interaction, which might be crucial for having Apaf1 at a threshold level needed for physiological apoptosis in developing neurons.

This work investigated the interaction between Ku and Apaf1 promoter during DNA damage, when cell survival response of DNA damage process is activated. Indeed, Ku has been reported as being involved in several processes, such as in the DNA repair pathway of NHEJ recombination, in silencing telomeres, in apoptosis and in gene transcription regulation.[19] As regards the DNA repair process, it is well known that Ku directly binds the free ends of the double-stranded DNA and recruits the DNA-PKcs and other repair factors, thus promoting numerous signalling pathways.[19] The finding that Ku and Apaf1 promoter could interact with the result of Apaf1 repression led us to hypothesise a possible function of this binding during the DNA repair process. We thus also explored the dynamics of Ku/Apaf1 promoter binding when DNA damage is induced upon genotoxic stress, this by using chromatin immunoprecipitation assay coupled to quantitative PCR. We discovered that Ku binds far more to the target sequence of Apaf1 promoter as soon as DNA damage is induced, when caspase 3 and apoptosis are not yet activated. This results in decreased Apaf1 levels, and suggests that the cell response to DNA damage is not only to repair the damage, but also to maintain lower the levels of at least one of the main apoptotic genes, Apaf1. Indeed, Apaf1 is

fundamental for the formation of the apoptosome, which is the core of the apoptotic programme and serves to activate executioner caspases, such as caspase 3.[5] It can be assumed that, when the damage to DNA becomes more severe and irreversibly unrepaired, Ku70/86 moves from Apaf1 promoter thus contributing to the apoptotic response. This idea is corroborated by the kinetics of Ku/Apaf1 promoter interaction that turns out to be comparable with the untreated cells at longer time points. Moreover, fluorescence microscopy analysis of nuclear 8-hydroxydeoxyguanosine (8-OHdG) content, a well-enstablished oxidative marker of DNA damage, indicated that it significantly increased to reach a plateau at 6 h of hydrogen peroxide treatment, without further rise at longer time points (see Supplementary Figure 3). Thus, the temporary association between 8-OHdG increase and Apaf1 upregulation argues for a causal relationship between the occurrence of an irreversible DNA damage and the release of Ku70/86 from Apaf1 promoter. This suggests that Apaf1 should be transcriptionally upregulated in order to promote apoptosome formation and caspase 3 activation.

Indeed, in such a stress-conditions, other players in the apoptosis pathway could be regulated by the cytosolic protein Ku70, such as the Bcl2-family member Bax. Bax is, in fact, sequestered from the mitochondria and deubiquitylated by Ku70 under normal conditions. Upon induction of apoptosis, Ku70 is acetylated thereby releasing Bax, which, in turn, translocates to the mitochondria and triggers cell death.[21] Therefore, we can speculate that the prompt release of cytochrome *c* observed upon hydrogen peroxide administration and in Ku-silenced cells, where both in untreated (Ctr) and treated cells (T1) is slightly more released into the cytosol (Figure 6a and c), is possibly due to Bax translocation to the mitochondria. In this perspective, Ku70/86-mediated modulation of Apaf1 expression upon DNA damage could mainly serve to delay the apoptotic process in order to allow DNA repair.

Also, we could hypothesize the possibility that p53, a well-known transcriptional activator of Apaf1[6–8] and a DNA damage-sensing protein,[36] could have a role in this regulation. In particular, after DNA damage induction, Ku70 and Ku86 form the huge DNA-PK complex with the DNA-PKcs, which in turn activates several pathways by the direct or indirect phosphorylation of different substrates, such as p53.[36] In this scenario, the upregulation of Apaf1 could be the result of both the Ku displacement from Apaf1 promoter and p53 binding.

The repression function of Ku on Apaf1 expression could reconcile the apparent conflicting observations, which indicate that Ku behaves as a tumour suppressor and oncoprotein.[37] In fact, as the impairment of DNA repair process produces genetic instability and, in turn, cancer development, it has been suggested that Ku's loss-of-function induces tumorigenesis.[38–40] Conversely, its gain-of-function has been associated with hyperproliferation and evading apoptosis of different tumour histotypes.[41,42] On the basis of the results obtained in this work, it could be speculated that the above-mentioned resistance phenomena are related to a Ku-dependent dysregulation of Apaf1 expression. Indeed, Apaf1 has been reported to be a potent tumour suppressor and drug resistance inducer.[43] Therefore, the identification of factors modulating Apaf1 expression, such as Ku itself,

may be highly relevant in the development of novel anticancer therapeutic agents.

Materials and Methods

Plasmids constructs. A region of about 7 kb of the murine Apaf1 promoter was obtained with PCR from a Bac (bacterial artificial chromosome) clone as template, with the primers: 5′-AAGCTTCACCTTTAGTCCCAGCA-3′ and 5′-AA GCTTTGTGCCTCAGGGTTTTCTC-3′. This region was cloned into the HindIII site of pGL3-basic vector (expressing Firefly luciferase) (Promega, Madison, WI, USA), generating the −4210 construct, from which the Δ −1509, Δ −589 and Δ +305 deletion constructs were created using the sites for Nhel-EcoRV, Xhol and Kpnl, respectively. A series of successive deletions (Δ −1402, Δ −1351, Δ −1287, Δ −1257, Δ −1202, Δ −1027 and Δ −903) was generated by PCR using −4210 construct as template and cloning them into the Nhel-AatII sites.

For the deletion constructs the reverse oligonucleotide was 5′-AGTGAGA CGTCTG CTCCT-3′; whereas the forward oligonucleotides were the following: (1) 5′-ATG CTAGCTGGGTTGTATGTGTCATAC-3′, (2) 5′-ATGCTAGCAGTACTA GGGAGGT GGAGGC-3′, (3) 5′-ATGCTAGCTGAGTTCAAGGACAGCC-3′, (4) 5′-ATGCTAGCAC AGGAGAAACCCTGTATCAAA-3′, (5) 5′-ATGCTAGCAATGTT TAGTCTTAAGGGA-3′, (6) 5′-ATGCTAGCTCTCTTGCGGGATCCTC-3′ and (7) 5′-ATGCTAGCTCTAAA TAGGAGAAAGTCTC-3′.

The construct pCMV-pGL3-basic was generated cloning the CMV promoter upstream the luciferase cDNA into the BglII–Spel sites.

The constructs E1Δ −589, E2Δ −589 and E1pCMV were generated by cloning the double-stranded oligonucleotides (obtained by annealing for 5 min at 95°C and overnight at RT) E1 and E2 (5′-ATTTACACTAATATATCACTAATATATGCTT GGTTTCAAAGCTACAAAT-3′ and 5′-GATATCCAGAGTCTTTTCTGAATTCTAT TAGCTCTCTTATTCCAC-3′) upstream of the promoters in Δ −589 and pCMV-pGL3-basic constructs, using the sites for BglII and BglII–Spel, respectively.

The plasmid containing the full-length form of mouse Ku70 (pKu70), cloned upstream the p3XFLAG-CMV-10 (Sigma-Aldrich Inc., St. Louis, MO, USA), was a kind gift of Dr Yasushi Enokido from Tokyo University. pKu86 was obtained by PCR cloning of the full-length mouse Ku86 cDNA between the sites NotI and BamHI (modified to blunt end) of p3XFLAG-CMV-10 vector. As regards pApaf1 expressing vector see.[32]

Cell cultures and transfections. The following cell lines were used in this study: ImimPc-2 (human pancreatic tumoral cells), ETNA (embryonic telencephalic naive Apaf1 cells), $B_{16}F_{10}$ (murine melanoma cells) and $C_3H_{10}T_{1/2}$ (murine fibroblasts). They were grown in DMEM (Sigma-Aldrich Inc.) containing 10% fetal bovine serum (FBS, Sigma-Aldrich Inc.), 100 U/ml penicillin and 100 μg/ml streptomycin, in a humidified atmosphere of 5% CO_2 at 37°C (except for ETNA cells, which were grown at 33°C). Transient siRNA transfection was performed with smart pool siRNA directed against four Ku70 mRNA sequences (siKu70), specific for mouse or human (Dharmacon RNA technologies, Lafayette, CO, USA). Their sequences are available on request. Control cells were transfected with a scramble siRNA duplex (Ambion, Foster City, CA, USA), which does not present homology with any other murine or human mRNAs. Transient expression of siRNA and of each vector was obtained with Lipofectamine2000 (Invitrogen, Carlsbad, CA, USA), according to the manufacturer's instructions. After 4 h incubation with transfection reagents, the cells were cultured in normal growth medium for the indicated period of time.

Cell treatments. ETNA cells were treated with apoptotic stimulus etoposide (Sigma-Aldrich Inc.) at a concentration of 20 μM for 1, 3, 6, 9, 12 and 24 h; hydrogen peroxide (Sigma-Aldrich Inc.) at a concentration of 500 μM for 1 h and then replaced with fresh medium for 1, 3, 6, 12 and 24 h; and staurosporine (Gibco, Carlsbad, CA, USA) at a concentration of 250 nM for 1, 3, 6 and 24 h.

Luciferase assay. ImimPc-2, ETNA, $B_{16}F_{10}$ and $C_3H_{10}T_{1/2}$ cells were co-transfected with one of the constructs, described above, containing the firefly luciferase and a pRL-TK plasmid that expresses the renilla luciferase, which is used as an internal control of the transfection efficiency. At 24 or 48 h after transfection, cells were harvested and analysed by using Dual-luciferase reporter assay system (Promega). The relative luciferase activity was calculated as the ratio between the firefly luciferase activity and the renilla luciferase activity.

Real-time PCR. RNA was isolated by using RNeasy Micro Kit (Qiagen Inc., Valencia, CA, USA), according to the manufacturer's instructions. For reverse transcriptase reaction, first strand cDNA was synthesized with esa primers by adding 1 μg of RNA with M-MLV reverse transcriptase (Invitrogen). Real-time PCR was performed by using SensiMix Plus SYBR Kit (Quantace Ltd., London, UK). Primers used are the following: mouse Apaf1 forward (N-ter) 5′-GTTCAAA GCCGAGACAGGAG-3′; mouse Apaf1 reverse (N-ter) 5′-ATTGACTTGCTCCGA GTGCT-3′; mouse Apaf1 forward (C-ter) 5′-GCTTGTCTCTGCTGGAGGATA-3′; mouse Apaf1 reverse (C-ter) 5′-GTCTGTGAGGAGTCCCCAGT-3′; human Apaf1 forward 5′-AACCAGGATGGGTCACCATA-3′; human Apaf1 reverse 5′-ACTGAAA CCCAATGCACTCC-3′. Real-time quantitation was performed by using a Fast-Real-Time PCR System (Applied Biosystems, Foster City, CA, USA). Data were normalized to β-actin or to GAPDH. For exogenous Apaf1 mRNA analysis, the normalization was performed with a pGFP plasmid co-transfected together with pApaf1. Fold-change was determined by using the $2^{-\Delta\Delta CT}$ method. All reactions were performed in triplicate.

Immunoblotting. After rinsing the cultures with ice-cold PBS, cell lysis was performed in RIPA buffer (50 mM Tris-HCl pH 7.4, 1% Triton X-100, 150 mM NaCl, 0.25% sodium deoxycholate, 0.1% SDS, 1 mM EDTA, 5 mM $MgCl_2$) and a protease inhibitor cocktail (Sigma, St. Louis, MO, USA). A clear supernatant was obtained by centrifugation of lysates at 17 000 g for 10 min. Alternatively, in order to obtain nuclear extracts cells were collected and incubated with 'nucleus buffer' (1 mM K_2HPO_4, 14 mM $MgCl_2$, 150 mM NaCl, 1 mM EGTA, 0.1 mM DTT, 0.3% Triton X-100, pH 6.4) for 30 min at 4°C, then centrifuged at 450 g for 10 min in order to isolate nuclei (pellet) from cytosolic fraction (supernatant). Pellet was finally lysed in RIPA buffer (50 mM Tris-HCl pH 7.4, 1% Triton X-100, 150 mM NaCl, 0.25% sodium deoxycholate, 0.1% SDS, 1 mM EDTA, 5 mM $MgCl_2$, protease and phosphatase inhibitors). Mitochondrion/cytosol fractionation was obtained by harvesting ETNA cells in hypotonic buffer (15 mM $MgCl_2$, 10 mM KCl, 10 mM Tris-MOPS, pH 7.4), supplemented with protease inhibitor cocktail and incubated for 15 min on ice. 1 Volume of 2 × Mitobuffer (400 mM sucrose, 10 mM TES, pH 7.2, 100 μM EGTA, 2 μM DTT) was added and the cell suspension was homogenized for 40 strokes with a Dounce homogenizer. Samples were centrifuged twice at 900 g for 10 min at 4°C to eliminate cell nuclei and unbroken cells. The resulting supernatant was centrifuged at 12 000 g for 15 min at 4°C to recover the heavy-membrane pellet enriched of mitochondria, and the resulting supernatant was stored as cytosolic fraction. Protein content was determined using Bradford protein assay (Bio-Rad, Hercules, CA, USA). Immunoblots were performed on polyvinylidene difluoride membranes (Immobilon P, Millipore, Billerica, MA, USA). Apaf1 was detected with a rat polyclonal anti-Apaf1 antibody (clone 18H2, Apotech Corp., Lausen, SW, USA) and was used at a concentration of 1 : 1000. The Ku70 or Ku86 were detected with a goat polyclonal anti-Ku70 or anti-Ku86 antibody (clone C-19 or M-20, Santa Cruz Biotechnology, Santa Cruz, CA, USA) at a concentration of 1 : 500. The H2B antibody was detected with a rabbit polyclonal anti-H2B (FL-126, Santa Cruz Biotechnology), which recognizes the histone 2B, at a concentration of 1 : 500. Cleaved active fragment of caspase 3 was detected by using a rabbit polyclonal anti-cleaved caspase-3 antibody at a concentration of 1 : 1000 (Cell Signaling, Danvers, MA, USA). Anti-γH2A.X antibody (clone JBW301, Millipore) was used at a concentration of 1 : 1000. Anti-cytochrome c monoclonal antibody (clone 7H8.2C12, BD Biosciences, San Jose, CA, USA) and anti-Cu/Zn SOD (SOD1) polyclonal antibody (Assay Designs, Ann Arbor, MI, USA) were used at concentration of 1 : 1000. Anti-OxPhos Complex I 39 kDa subunit antibody (clone 20C11, Invitrogen) was used at concentration of 1 : 2000. Anti-β-actin (clone AC15) antibody was purchased from Sigma-Aldrich Inc. (1 : 3000 diluted).

EMSA. EMSA was performed using E1 double-stranded oligonucleotide (5′-AT TTACACTAATATATCACTAATATATGCTTGGTTTCAAAGCTACAAAT-3′), corresponding to the region located between −1509 and −1402 nucleotides of the Apaf1 promoter. The oligonucleotide was end-labeled using (γ-^{32}P) ATP. Nuclear extracts were prepared as follows: 10^7 cells were centrifuged at 1000 r.p.m. for 5 min, the pellet was resuspended in buffer H (10 mM HEPES pH 7.9, 50 mM NaCl, 0.5 M sucrose, 0.1 mM EDTA, 0.5% Triton, 1 mM DTT, 1 mM PMSF) and incubated on ice for 5 min. After centrifugation at 1000 r.p.m. for 10 min, pellet was washed in buffer A (10 mM HEPES pH 7.9, 10 mM KCl, 0.1 mM EDTA, 0.1 mM EGTA, 1 mM DTT). Then it was resuspended in buffer C (10 mM HEPES pH 7.9, 500 mM NaCl, 0.1 mM EDTA, 0.1% IGEPAL, 1 mM DTT) and vortexed for 10 min at 4°C. The sample was centrifuged at 13 000 r.p.m. for 5 min and the supernatant was stored at −80°C. Protein concentration was determined by Bradford protein assay (Bio-Rad).

The extracts were preincubated for 5 min at RT in presence of poly (dI-dC) (Amersham, Buckinghamshire, UK) to reduce aspecific bindings. The reaction was performed at RT for 20 min in binding buffer (50% glycerol, 250 mM KCl, 100 mM HEPES, 1 mM DTT, 5 mg/ml BSA) using 5 μg of nuclear extracts and 20 cpm oligonucleotides. Samples were loaded on a non-denaturing 6% polyacrylamide gel in 0.25 × TBE (Tris-borate-EDTA buffer) for 2 h at 4°C. The radioactive signals were detected using the Storm Imager (Amersham).

DNA pull-down assay. Streptavidin magnetic beads (Promega) were washed three times with Buffer A (5 mM Tris pH 8, 0.5 mM EDTA, 1 M NaCl). Annealed E1 oligonucleotide (biotin-labelled) was incubated with beads for 15 min at RT in buffer A. Beads were then washed twice with buffer A and resuspended in buffer C (5 mM Tris pH8, 1 mM EDTA, 1 mM DTT, 50 mM NaCl). Nuclear proteins, extracted by a nuclear extraction kit (Active Motif, Carlsbad, CA, USA), were incubated with beads bound to the oligonucleotide E1 or to a negative control oligonucleotide (5′-GGGGTTGTATGTGTCATACAGCCAGGTT-3′), washed twice with buffer C and eluted in 1 M NaCl or by using oligonucleotide competition. Eluted proteins were analysed by SDS-PAGE and stained with SYPRO Ruby (Bio-Rad).

In-gel tryptic digestion and MALDI-TOF/TOF analysis. Bands were excised from the gels with an automatic spot picker (Investigator ProPic, Genomic Solutions Inc.) and subjected to in-gel tryptic digestion. In brief, gel bands were destained with 50%ACN in 50 mM ammonium bicarbonate. Then, the gel bands were shrunk by addition of 100%ACN. The dried gel pieces were reswollen with 4.5 ng/ml trypsin in 50 mM ammonium bicarbonate and digested overnight at 37°C. Peptides were concentrated with ZipTip μC18 pipette tips (Millipore). Co-elution was performed directly onto a MALDI target with 1 μl of a-cyano-4-hydroxycinnamic acid matrix (5 mg/ml in 50% acetonitrile, 0.1% TFA). MALDI-MS and MALDI-MS/MS were performed on an Applied Biosystems 4700 Proteomics Analyzer with TOF/ TOF ion optics. The spectra were acquired in the positive reflector mode by 40 subspectral accumulations (each consisting of 50 laser shots) in a 800–4000 mass range, focus mass 2100 Da, using a 355 nm Nb:YAG laser with a 20 kV acceleration voltage. Peak labeling was automatically done by 4000 series explorer software Version 3.0 (Applied Biosystems) considering only peaks that exceeded a signal-to-noise ratio of 10 (local noise window 200 *m/z*) and a half maximal width of 2.9 bins. Calibration was performed using peptides resulting from autoproteolysis of trypsin (*m/z* – 842.510, 1045.564, 2211.105, 2239.136 and 2807.300). In addition to peptide mass finger spectra, the five most abundant precursor ion masses having a signal-to-noise ratio higher than 50 were chosen for MS/MS fragmentation. MS/MS spectra were integrated over 1500 laser shots in the 1 kV positive ion mode. Air at the medium gas pressure setting (1.25×10^{-6} torr) was used as the collision gas in the CID off mode. The interpretation of both the MS and MS/MS data were carried out with the GPS Explorer software (Version 3.6, Applied Biosystems). Peaks were extracted from raw spectra by the GPS software using the following setting: MS peak filtering – mass range: 800–4000 Da; minimum signal-to-noise ratio: 10. MS/MS peak filtering – mass range: 60–20 Da below precursor mass; minimum signal-to-noise ratio: eight. An exclusion list of known contaminant ion masses of keratin and trypsin was used. A combined MS peptide fingerprint and MS/MS peptide sequencing search was performed against the NCBI nonredundant database without taxon restriction using the MASCOT search algorithm. These searches specified trypsin as the digestion enzyme, carbamidomethylation of cysteine as fixed modification, partial oxidation of methionine and phosphorylation of serine, threonine and tyrosine as variable modifications, and allowed for one missed trypsin cleavage. The monoisotopic precursor ion tolerance was set at 30–50 ppm and the MS/MS ion tolerance at 0.3 Da. Protein identifications were accepted with a statistically significant MASCOT protein search score ≥ 76 that corresponded to an error probability of $P < 0.05$ in our data set. MS/MS peptide spectra with a minimum ion score confidence interval $\geq 95\%$ were accepted. This was equivalent to a median ion score cut off of approximately 35 in the data set. The raw mass spectra were exported to an Excel file, combined with the peak annotations and modification information for identified peptides obtained with the GPS explorer (Supplementary File: Mass Spectrometry Data.xls). Peaks subjected to MS/MS analysis are indicated together with their median ion score.

ChIP assay and quantitative PCR. ETNA cells, grown in 150-mm dishes, were cross-linked by incubating with fixing solution (1% formaldehyde, 10 mM NaCl, 0.1 mM EDTA, 50 μM EGTA, 5 mM HEPES pH 8.0, 10 mM PMSF) for 10 min at RT. Crosslinking was halted by adding 0.125 M glycine for 5 min. Then, cells were washed three times in ice-cold PBS, resuspended in ice-cold cell lysis buffer (5 mM PIPES pH 8.0, 85 mM KCl, 0.5% NP40, 1 mM PMSF, 1X protease inhibitors) and incubated on ice for 10 min. The nuclei were pelleted at 2000 g for 5 min at 4°C and then, suspended in ice-cold nuclear lysis buffer (50 mM Tris-HCl pH 8.0, 10 mM EDTA, 0.8% SDS, 1 mM PMSF, 1X protease inhibitors) and incubated for 30 min on ice. Chromatin was sonicated in the presence of glass beads (150–200 mm, Sigma-Aldrich Inc.) with pulses of 30 s at 80% of amplitude, centrifuged for 10 min at 4°C at 14 000 g, diluted four times with dilution buffer (10 mM Tris-HCl pH 8.0, 0.5 mM EGTA, 1% Triton X-100, 140 mM NaCl, 1 mM PMSF, protease inhibitors), then quantified by using the Nanodrop Spectrophotometer ND-1000 and stored at −80°C. For each immunoprecipitation, equal amount of chromatin was diluted with RIPA buffer (10 mM Tris-HCl pH 8.0, 1 mM EDTA, 0.5 mM EGTA, 1% Triton X-100, 0.1% Na-Deoxycholate, 0.1% SDS, 140 mM NaCl, 1 mM PMSF) to same volume and precleared by incubation with 20 μl of Protein A/G agarose beads (Santa Cruz Biotechnology) for 2 h at 4°C. After preclearing, samples were centrifuged for 10 min at 14000 g at 4°, and then incubated overnight at 4°C with the primary antibody. We used 6 μg of anti-Ku70/86 (clone 162, LabVision/Neomarkers Fremont, CA, USA) or 4 μg of anti-RNA Poymerase II (clone CTD4H8, Abcam, Cambridge, MA, USA) or without antibody as negative control. Antibody-Ku or -Pol II complexes were recovered by incubating with 20 μl of Protein A/G agarose beads for 4 h at 4°C. Beads were centrifuged for 10 min at 14 000 g at 4°C and, before washing, the supernatant of the no-antibody control was transferred in a new tube and left on ice, as total input control. Beads were washed five times with RIPA buffer, once with LiCl buffer (0.25 M LiCl, 0.5% NP 40, 0.5% Na-Deoxycholate, 1 mM Na-EDTA, 10 mM Tris-HCl pH 8.0), and once with TE (1 mM EDTA, 10 mM Tris-HCl pH 8.0). Then, beads were resuspended in TE and RNase cocktail enzyme mix (Applied Biosystems) was added to each samples, including to input control. After 30 min at 37°C of RNase reaction, cross-linking was reversed by the incubation at 65°C overnight, and protein complexes were degraded with the addition of 0.5 μg/ml proteinase K (Sigma-Aldrich Inc.) and 0.5% SDS at 50°C for 3 h. DNA was recovered with Phenol/Chloroform extraction followed by ethanol precipitation and resuspended in 30 μl TE.

Quantitative real-time PCR was performed by using 1 μl DNA. Data were normalized to the input and calculated as $2^{-\Delta CT}$, and the obtained values were related to the no-antibody condition ($\Delta 2^{-\Delta CT}$). All reactions were performed in triplicate. Primers used to amplify the Apaf1 repressing region are forward: 5′-CCT GGAGGATATCCAGAGTC-3′ or 5′-TGTCTGGTGTCTTACAACCATTG-3′, reverse: 5′-CATCCCGCTCAACATTTGTA-3′ or 5′-GTTCGTTGTTGCTGAGCGATAAA-3′. Primers used to amplify the transcription start point (TSP) region are forward: 5′-CT GGGCGAGTGAATTTGC-3′ and reverse: 5′-AGACGTCTGCTCCTCTAGCTG-3′. Primers used to amplify the glucose-6-phosphate dehydrogenase X-linked (G6pdx) gene are forward: 5′-AGACTAGCCCGAAGCTCCTC-3′ and reverse: 5′-TCAGACC ACCCCTTTACCTG-3′.

Analysis of cell viability and apoptosis. Adherent and detached cells were combined and stained with 50 μg/ml propidium iodide before analysis by a FACScalibur instrument (BD Biosciences). Apoptotic cells were evaluated by calculating peak areas of hypodiploid nuclei in previously premeabilized cells (sub-G1).

Immunofluorescence. ETNA cells, grown in 35-mm Petri dishes, were washed in PBS and then fixed with 4% paraformaldehyde in PBS for 30 min. After permeabilization with 0.4% Triton X-100 in PBS for 5 min, cells were blocked in 3% bovine serum albumin (BSA) or 10% normal goat serum (NGS) in PBS for 30 min and incubated over night at 4°C with anti-γH2A.X or with anti-8-OHdG primary antibodies (clone JBW301, Millipore; clone 15A3, QED Biosciences Inc., San Diego, CA, USA), in 1% BSA or 2% NGS and 0,4% Triton X-100. Cells were then washed in PBS and incubated for 1 h with Alexa Fluor 488-conjugated goat anti-mouse (Molecular Probes). After rinsing in PBS, cell nuclei were stained with 1 μg/ml DAPI and observed by confocal microscopy with a Leica TSC-SPE confocal microscope equipped with a 63 × /1.15 Olympus objective and a Leica Application Suite (LAS) software (Leica Microsystems, Wetzlar, Germany). Fluorescence images were adjusted for brightness, contrast and colour balance by using Adobe Photoshop CS (San Jose, CA, USA).

Densitometric analyses of fluorescence images. Quantification of the changes in the immunoreactivity of 8-OHdG signal because of different times of hydrogen peroxide incubation (ctr, T3, T6 and T24) was performed on 8-OHdG-positive nuclei by densitometric analyses. 8-OHdG-positive nuclei associated signals were quantified by manually outlining individual nuclei and measuring nuclear associated fluorescence intensity with the ImageJ software

(http://rsb.info.nih.gov/ij/). The ratio, F/A, defines mean fluorescence of individual nuclei (F) normalized to total nuclear surface (A). Quantification was done on 30 cells per field, at least 6 fields ($n = 6$) for each time point.

Data presentation. All experiments were performed at least three different times, unless otherwise indicated. Data are expressed as the means $\pm$ S.D. or S.E.M. and significance was assessed by Student's *t* test. Differences with *P*-values < 0.05 were considered as significant.

Conflict of interest

The authors declare no conflict of interest.

1. Kim HE, Du F, Fang M, Wang X. Formation of apoptosome is initiated by cytochrome c-induced dATP hydrolysis and subsequent nucleotide exchange on Apaf-1. *Proc Natl Acad Sci USA* 2005; **102**: 17545–17550.
2. Acehan D, Jiang X, Morgan DG, Heuser JE, Wang X, Akey CW. Three-dimensional structure of the apoptosome: implications for assembly, procaspase-9 binding, and activation. *Mol Cell* 2002; **9**: 423–432.
3. Reubold TF, Wohlgemuth S, Eschenburg S. A new model for the transition of APAF-1 from inactive monomer to caspase-activating apoptosome. *J Biol Chem* 2009; **284**: 32717–32724.
4. Bao Q, Shi Y. Apoptosome: a platform for the activation of initiator caspases. *Cell Death Differ* 2007; **14**: 56–65.
5. Boatright KM, Salvesen GS. Mechanisms of caspase activation. *Curr Opin Cell Biol* 2003; **15**: 725–731.
6. Fortin A, Cregan SP, MacLaurin JG, Kushwaha N, Hickman ES, Thompson CS *et al.* APAF1 is a key transcriptional target for p53 in the regulation of neuronal cell death. *J Cell Biol* 2001; **155**: 207–216.
7. Kannan K, Kaminski N, Rechavi G, Jakob-Hirsch J, Amariglio N, Givol D. DNA microarray analysis of genes involved in p53 mediated apoptosis: activation of Apaf-1. *Oncogene* 2001; **20**: 3449–3455.
8. Moroni MC, Hickman ES, Lazzerini Denchi E, Caprara G, Colli E, Cecconi F *et al.* Apaf-1 is a transcriptional target for E2F and p53. *Nat Cell Biol* 2001; **3**: 552–558.
9. Rozenfeld-Granot G, Krishnamurthy J, Kannan K, Toren A, Amariglio N, Givol D *et al.* A positive feedback mechanism in the transcriptional activation of Apaf-1 by p53 and the coactivator Zac-1. *Oncogene* 2002; **21**: 1469–1476.
10. Furukawa Y, Nishimura N, Satoh M, Endo H, Iwase S, Yamada H *et al.* Apaf-1 is a mediator of E2F-1-induced apoptosis. *J Biol Chem* 2002; **277**: 39760–39768.
11. Furukawa Y, Sutheesophon K, Wada T, Nishimura M, Saito Y, Ishii H. Methylation silencing of the Apaf-1 gene in acute leukemia. *Mol Cancer Res* 2005; **3**: 325–334.
12. Peltenburg LT, de Bruin EC, Meersma D, Smit NP, Schrier PI, Medema JP. Expression and function of the apoptosis effector Apaf-1 in melanoma. *Cell Death Differ* 2005; **12**: 678–679.
13. Soengas MS, Capodieci P, Polsky D, Mora J, Esteller M, Opitz-Araya X *et al.* Inactivation of the apoptosis effector Apaf-1 in malignant melanoma. *Nature* 2001; **409**: 207–211.
14. Teodoridis JM, Hall J, Marsh S, Kannall HD, Smyth C, Curto J *et al.* CpG island methylation of DNA damage response genes in advanced ovarian cancer. *Cancer Res* 2005; **65**: 8961–8967.
15. Wallace DM, Cotter TG. Histone deacetylase activity in conjunction with E2F-1 and p53 regulates Apaf-1 expression in 661W cells and the retina. *J Neurosci Res* 2009; **87**: 887–905.
16. Wright KM, Smith MI, Farrag L, Deshmukh M. Chromatin modification of Apaf-1 restricts the apoptotic pathway in mature neurons. *J Cell Biol* 2007; **179**: 825–832.
17. Johnson CE, Huang YY, Parrish AB, Smith MI, Vaughn AE, Zhang Q *et al.* Differential Apaf-1 levels allow cytochrome c to induce apoptosis in brain tumors but not in normal neural tissues. *Proc Natl Acad Sci USA* 2007; **104**: 20820–20825.
18. Lieber MR, Ma Y, Pannicke U, Schwarz K. Mechanism and regulation of human non-homologous DNA end-joining. *Nat Rev Mol Cell Biol* 2003; **4**: 712–720.
19. Downs JA, Jackson SP. A means to a DNA end: the many roles of Ku. *Nat Rev Mol Cell Biol* 2004; **5**: 367–378.
20. Mimori T, Akizuki M, Yamagata H, Inada S, Yoshida S, Homma M. Characterization of a high molecular weight acidic nuclear protein recognized by autoantibodies in sera from patients with polymyositis-scleroderma overlap. *J Clin Invest* 1981; **68**: 611–620.
21. Amsel AD, Rathaus M, Kronman N, Cohen HY. Regulation of the proapoptotic factor Bax by Ku70-dependent deubiquitylation. *Proc Natl Acad Sci USA* 2008; **105**: 5117–5122.
22. Mo X, Dynan WS. Subnuclear localization of Ku protein: functional association with RNA polymerase II elongation sites. *Mol Cell Biol* 2002; **22**: 8088–8099.
23. Sucharov CC, Helmke SM, Langer SJ, Perryman MB, Bristow M, Leinwand L. The Ku protein complex interacts with YY1, is up-regulated in human heart failure, and represses alpha myosin heavy-chain gene expression. *Mol Cell Biol* 2004; **24**: 8705–8715.
24. Nolens G, Pignon JC, Koopmansch B, Elmoualij B, Zorzi W, De Pauw E *et al.* Ku proteins interact with activator protein-2 transcription factors and contribute to ERBB2 overexpression in breast cancer cell lines. *Breast Cancer Res* 2009; **11**: R83.
25. Errami A, Smider V, Rathmell WK, He DM, Hendrickson EA, Zdzienicka MZ *et al.* Ku86 defines the genetic defect and restores X-ray resistance and V(D)J recombination to complementation group 5 hamster cell mutants. *Mol Cell Biol* 1996; **16**: 1519–1526.
26. Gu Y, Jin S, Gao Y, Weaver DT, Alt FW. Ku70-deficient embryonic stem cells have increased ionizing radiosensitivity, defective DNA end-binding activity, and inability to support V(D)J recombination. *Proc Natl Acad Sci USA* 1997; **94**: 8076–8081.
27. Singleton BK, Priestley A, Steingrimsdottir H, Gell D, Blunt T, Jackson SP *et al.* Molecular and biochemical characterization of xrs mutants defective in Ku80. *Mol Cell Biol* 1997; **17**: 1264–1273.
28. Bonner WM, Redon CE, Dickey JS, Nakamura AJ, Sedelnikova OA, Solier S *et al.* GammaH2AX and cancer. *Nat Rev Cancer* 2008; **8**: 957–967.
29. Lan L, Nakajima S, Oohata Y, Takao M, Okano S, Masutani M *et al. In situ* analysis of repair processes for oxidative DNA damage in mammalian cells. *Proc Natl Acad Sci USA* 2004; **101**: 13738–13743.
30. Margaritis T, Holstege FC. Poised RNA polymerase II gives pause for thought. *Cell* 2008; **133**: 581–584.
31. Saunders A, Core LJ, Lis JT. Breaking barriers to transcription elongation. *Nat Rev Mol Cell Biol* 2006; **7**: 557–567.
32. Cozzolino M, Ferraro E, Ferri A, Rigamonti D, Quondamatteo F, Ding H *et al.* Apoptosome inactivation rescues proneural and neural cells from neurodegeneration. *Cell Death Differ* 2004; **11**: 1179–1191.
33. Hediger F, Neumann FR, Van Houwe G, Dubrana K, Gasser SM. Live imaging of telomeres: yKu and Sir proteins define redundant telomere-anchoring pathways in yeast. *Curr Biol* 2002; **12**: 2076–2089.
34. Cecconi F, Alvarez-Bolado G, Meyer BI, Roth KA, Gruss P. Apaf1 (CED-4 homolog) regulates programmed cell death in mammalian development. *Cell* 1998; **94**: 727–737.
35. Gu Y, Sekiguchi J, Gao Y, Dikkes P, Frank K, Ferguson D *et al.* Defective embryonic neurogenesis in Ku-deficient but not DNA-dependent protein kinase catalytic subunit-deficient mice. *Proc Natl Acad Sci USA* 2000; **97**: 2668–2673.
36. Kruse JP, Gu W. Modes of p53 regulation. *Cell* 2009; **137**: 609–622.
37. Gullo C, Au M, Feng G, Teoh G. The biology of Ku and its potential oncogenic role in cancer. *Biochim Biophys Acta* 2006; **1765**: 223–234.
38. Li GC, Ouyang H, Li X, Nagasawa H, Little JB, Chen DJ *et al.* Ku70: a candidate tumor suppressor gene for murine T cell lymphoma. *Mol Cell* 1998; **2**: 1–8.
39. Pucci S, Mazzarelli P, Rabitti C, Giai M, Gallucci M, Flammia G *et al.* Tumor specific modulation of KU70/80 DNA binding activity in breast and bladder human tumor biopsies. *Oncogene* 2001; **20**: 739–747.
40. Tong WM, Cortes U, Hande MP, Ohgaki H, Cavalli LR, Lansdorp PM *et al.* Synergistic role of Ku80 and poly(ADP-ribose) polymerase in suppressing chromosomal aberrations and liver cancer formation. *Cancer Res* 2002; **62**: 6990–6996.
41. Klein A, Miera O, Bauer O, Golfier S, Schriever F. Chemosensitivity of B cell chronic lymphocytic leukemia and correlated expression of proteins regulating apoptosis, cell cycle and DNA repair. *Leukemia* 2000; **14**: 40–46.
42. Lim JW, Kim H, Kim KH. Expression of Ku70 and Ku80 mediated by NF-kappa B and cyclooxygenase-2 is related to proliferation of human gastric cancer cells. *J Biol Chem* 2002; **277**: 46093–46100.
43. Schafer ZT, Kornbluth S. The apoptosome: physiological, developmental, and pathological modes of regulation. *Dev Cell* 2006; **10**: 549–561.

Supplementary Information accompanies the paper on Cell Death and Differentiation website (http://www.nature.com/cdd)